Chen, C., Zhang, X., Groll, E., McKibben, A., Long, N., Dexter, M., and Chen, Q. 2016. "A method of assessing the energy cost saving from using an effective door closer," *Energy and Buildings*, 118: 329–338.

A Method of Assessing the Energy Cost Saving from Using an Effective Door Closer

Chun Chen[1,2], Xinye Zhang[1], Eckhard Groll[1], Aaron McKibben[4], Nicholas Long[4], Matthew Dexter[4], and Qingyan Chen[3,1*]

[1] School of Mechanical Engineering, Purdue University, West Lafayette, IN 47907, USA
[2] Department of Mechanical and Automation Engineering, The Chinese University of Hong Kong, Shatin, N.T. 999077, Hong Kong SAR, China
[3] Tianjin Key Laboratory of Indoor Air Environmental Quality Control, School of Environmental Science and Engineering, Tianjin University, Tianjin 300072, China
[4] Allegion plc, Carmel, IN 46032, USA
[*] Phone: (765) 496-7562, Fax: (765) 496-0539, Email: yanchen@purdue.edu

Abstract

Door closers are widely used for doors in commercial buildings, not only for safety purposes but also for reducing the airflow through door openings. This study aimed to develop a method for quickly assessing, in the design phase, the heating and cooling energy cost saving from using an effective door closer. The method developed in this study consists of a stop angle model, airflow model, and energy cost calculation. This investigation also conducted experimental measurements in a full-scale test facility to validate the models. This study then used the proposed method to assess the heating and cooling energy cost saving from using an effective door closer in the cities of Minneapolis, Boston, San Francisco, and Phoenix. It was found that, under a greater indoor-outdoor pressure differential, using an effective door closer would save more energy cost. When using a closer with a larger size, the energy cost lost would decrease, but a large closing torque may significantly reduce ease of use and accessibility and potentially violate building codes related to the Americans with Disabilities Act (ADA). Furthermore, the energy cost saving from using an effective door closer in San Francisco would be lower than that in Minneapolis, Boston, and Phoenix.

Keywords: Stop angle model; Pressure differential force; Airflow model; Discharge coefficient; Tracer gas measurement; Computational Fluid Dynamics.

1. Introduction

The building sector accounts for nearly 41% of the total primary energy consumption in the United States [1]. Therefore, energy saving in buildings has the potential to significantly reduce overall energy consumption. Air infiltration through the building envelope is considered to be among the most important factors in building energy saving [2-4]. The National Institute of Standards and Technology (NIST) has reported that annual heating and cooling energy costs could be reduced by 3% to 36% for different climate zones if the target air tightness level were achieved [5]. In commercial buildings where exterior doors are used frequently, airflow through door openings can cause a considerable increase in energy consumption. In strip malls with vestibules, for example, the total energy consumption is 5.61% lower than in similar malls without vestibules [6]. Therefore, building designers are paying more and more attention to the reduction of airflow through exterior door openings.

Door closers are widely used for doors in commercial buildings, not only for safety purposes but also for reducing the airflow through exterior door openings. Ease of use and accessibility are ongoing requisites for building designers and facilities management. The Americans with Disabilities Act (ADA) has set a maximum force for pushing or pulling open a door for accessibility reasons [7]. These requirements in turn limit the amount of force that can be applied by a door closer to close the door. When the indoor-outdoor pressure differential created by a ventilation system is relatively large, the door closer with low opening force set to accommodate ease of use may not be able to overcome the resistance and fully close the door. In this case, the door may remain open at the angle at which the force due to the pressure differential balances the closing force. Under such circumstances, the continuous airflow through the door opening could significantly increase the energy costs for heating and cooling.

During the design phase, designers must decide whether or not to use door closers in a building, and what kind of door closer to use. This decision for an effective door closer should help achieve a balance among accessibility, security, and energy efficiency. From the perspective of energy efficiency, designers need to know the extent to which heating and cooling energy costs can be reduced by the use of an effective door closer. However, there is no simple method available for obtaining such information in the design phase. In fact, a literature search found very few scientific publications focusing on door closers. Several studies have investigated the design of door closers [8,9] and their effectiveness in improving fire safety [10, 11], but these studies did not address the issue of energy efficiency. Therefore, the present study aimed to develop a method for quickly assessing, in the design phase, the heating and cooling energy cost saving from using an effective door closer.

The method developed in this study consists of (1) a model for determining the stop angle at which the pressure differential force balances the closing force produced by a door closer, (2) a model for calculating the airflow rate through a door opening that accounts for various influencing factors, and (3) energy calculation with the use of the two models. This study also conducted experimental measurements in a full-scale test facility to validate the two models. This investigation then used the proposed method to assess the heating and cooling energy

cost saving from using an effective door closer in different climate zones.

2. Methods

As discussed above, an ineffective door closer or closer with low opening force to accommodate ease of use may not be able to overcome the force on the door due to the indoor-outdoor pressure differential. In this case, a door may remain open at a certain angle, which could result in a significant increase in heating and cooling energy costs. This study first developed a model for determining the stop angle, θ^*, at which the pressure differential force balances the closing force produced by a door closer, as described in Section 2.1. Next, the stop angle was used to calculate the airflow rate through the door opening. This investigation then developed an airflow model for calculating the flow rate through a door opening that accounts for various influencing factors, as described in Section 2.2. The final step was to calculate the effect of the airflow rate through the door opening on heating and cooling energy costs. The energy cost calculation method is described in Section 2.3.

2.1 Stop angle model

The stop angle is the angle at which the door remains open when the pressure differential force balances the closing force produced by a door closer. Note that the force on the door due to the indoor-outdoor pressure differential depends on the opening angle. When the door is fully closed, this pressure force is equal to the indoor-outdoor pressure differential multiplied by the area of the door. When the door is opened to a certain degree, the pressure force on the door is smaller than the product of the pressure differential and the door area because of the drop in pressure. To correlate the pressure force on the door and the indoor-outdoor pressure differential, this study conducted numerical wind tunnel tests using computational fluid dynamics (CFD) and created a database. Figure 1 shows the configuration of the wind tunnel with a partially opened door that was used in the numerical tests. The wind tunnel had dimensions of 25 m in length, 6 m in width, and 3.5 m in height. The door was 2 m high and 0.9 m wide. The case setup was the same as that in a previous study by Yang et al. [12]. There were 45 cases with different door opening angles (10, 20, 30, 40, 50, 60, 70, 80, and 90^o) and inlet air velocities (0.2, 0.4, 0.6, 0.8, and 1 m/s). This study employed the RNG k-ε turbulence model to calculate the pressure distribution across the door opening, as shown in Figure 1. The CFD model was validated by experimental data measured by Yang et al. [12]. The pressure differentials between the two sides of the door, ΔP_{door}, and the corresponding indoor-outdoor pressure differentials, ΔP, for the 45 cases were recorded to create a database.

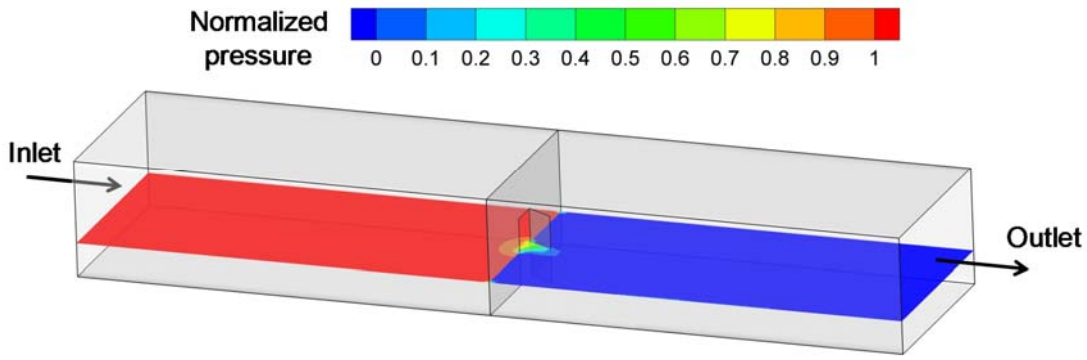

Figure 1. Calculated normalized pressure distribution at a height of 1 m in the numerical wind tunnel test when the opening angle was 60° and inlet velocity was 1 m/s. The pressure was normalized by the pressure at the inlet.

Figure 2 shows the ratio of ΔP_{door} to ΔP as a function of door opening angle. It can be seen that, for a given door opening angle, the five data points with different inlet velocities (0.2, 0.4, 0.6, 0.8, and 1 m/s) collapse to a single point. Therefore, the ratio of ΔP_{door} to ΔP is independent of the inlet velocity. However, the ratio of ΔP_{door} to ΔP decreases with the increase in door opening angle. Through a least-squares regression, the relationship between the ratio of ΔP_{door} to ΔP and the door opening angle can be expressed by

$$\frac{\Delta P_{door}}{\Delta P} = 1 - 0.0057\theta - 0.00006\theta^2 \quad (1)$$

where ΔP_{door} is the pressure differential between the two sides of the door (Pa), ΔP is the indoor-outdoor pressure differential (Pa), and θ is the door opening angle (°).

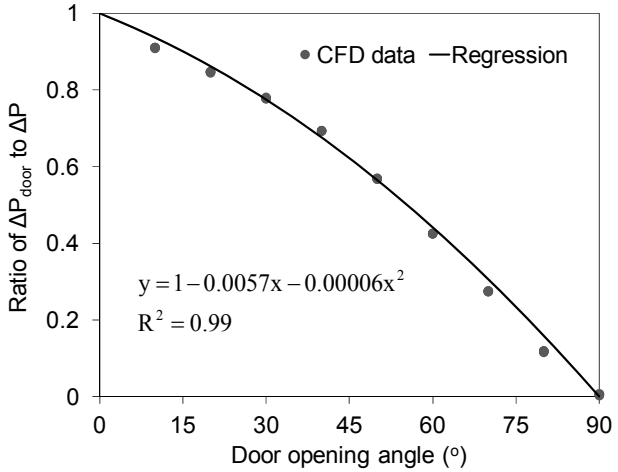

Figure 2. Relationship between the ratio of ΔP_{door} to ΔP and the door opening angle.

Note that the pressure differential quickly drops as the door is opened, because of the reduction in resistance. This has been verified by both our field tests and laboratory

measurements. To quantify the impact of the pressure drop, this study conducted measurements in a full-scale two-room test facility as shown in Figure 3. Room 1 was used to simulate the outdoor environment, and Room 2 to simulate the indoor environment. A door with dimensions of 2.1 m in height and 0.9 m in width was installed between the two rooms to simulate an exterior door that opens to the outside. A variable-speed fan system was used to exhaust air from Room 1, which created a pressure differential between the "indoor" and "outdoor" environments. For a fixed fan speed, the indoor-outdoor pressure differential when the door was fully closed, $\Delta P(0)$, was fixed. Under a given $\Delta P(0)$, the indoor-outdoor pressure differential, ΔP, as a function of door opening angle was measured using a manometer with an accuracy of 0.1 Pa.

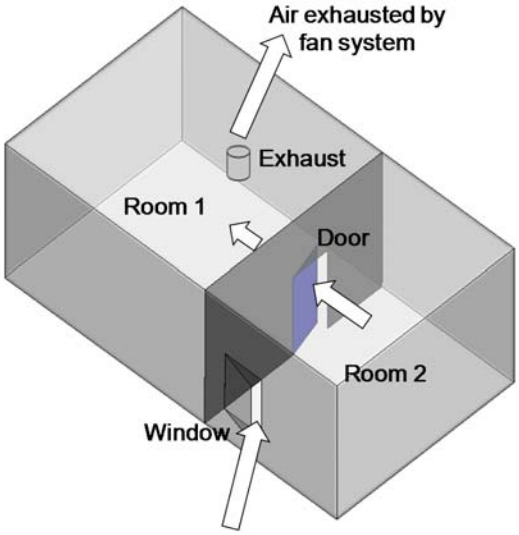

Figure 3. Schematic of the two-room test facility.

The measurement results indicated that the ratio of ΔP to $\Delta P(0)$ was independent of $\Delta P(0)$. On the other hand, the ratio of ΔP to $\Delta P(0)$ decreased with the increase in door opening angle. Figure 4 shows the relationship between the ratio of ΔP to $\Delta P(0)$ and the door opening angle, which can be expressed by the following equation through a least-squares regression:

$$\frac{\Delta P}{\Delta P(0)} = \begin{cases} -0.0729 \cdot \theta^2 - 0.0786 \cdot \theta + 1 & \theta < 2.5^o \\ 1.5357 \cdot \theta^{-1.4864} & \theta \geq 2.5^o \end{cases} \quad (2)$$

where $\Delta P(0)$ is the indoor-outdoor pressure differential when the door is fully closed.

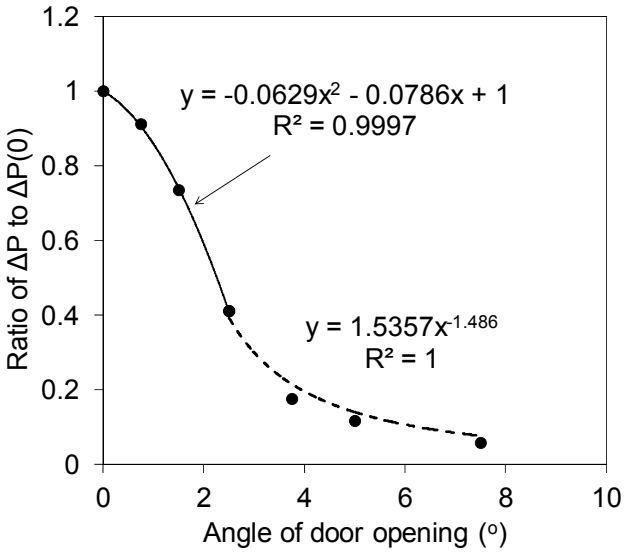

Figure 4. Relationship between the ratio of ΔP to ΔP(0) and the door opening angle.

When the friction and drag force are neglected, the closing force produced by a door closer balances the force due to the pressure differential. When the hinge is taken as the reference point, the torque balance can be obtained:

$$\tau_{\Delta P} = \Delta P_{door} A \cdot \frac{1}{2} W = \tau_{closer} \tag{3}$$

where $\tau_{\Delta P}$ is the torque due to the pressure differential (N·m), A is the area of the door (m^2), W is the width of the door (m), and τ_{closer} is the closing torque produced by the door closer (N·m). This study measured the closing torque produced by a door closer under a certain spring setting. The closer can be adjusted by turning a screw that preloads the springs inside the closer. Figure 5 shows the measured closing torque as a function of door opening angle under different spring settings. The closer sizes 0, 1, 2, and 3 designation represents an adjustment of the closer in which this screw was fully rotated 0, 3, 6, and 8 times, respectively, from the lower stop. Note that, according to the ADA standard for accessibility, less than 22 N of force should be required to open the door [7]. At the spring setting of closer size 1, the force required to open the door to 70° would typically be slightly less than 22 N. By contrast, the closer size 2 and closer size 3 settings will not meet the ADA standard and may not be desirable for ease of use and accessibility. The measured closing torque can be used as an input for the stop angle model. With a given indoor-outdoor pressure differential and closer spring setting, the stop angle, θ^*, can be obtained by solving Eqs. (1) to (3) together. Note that when the closing torque produced by the door closer is sufficiently large, there is no solution for the equations, which means that the door can be fully closed with the given torque.

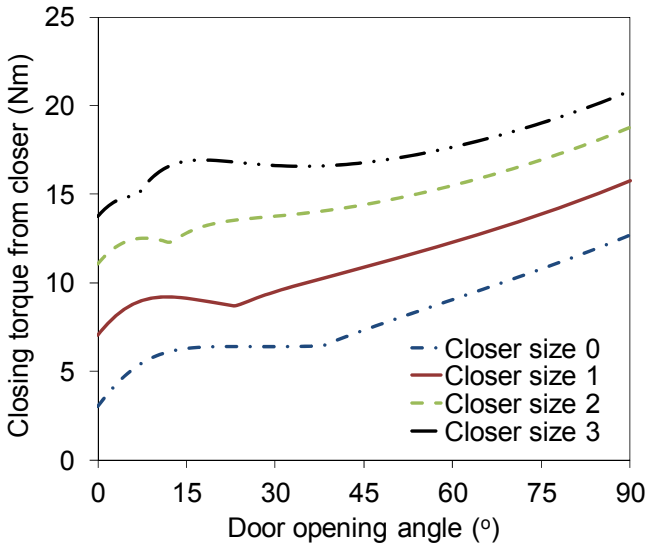

Figure 5. Measured closing torque as a function of door opening angle under different spring settings.

2.2 Airflow model

Once the stop angle has been obtained from the model described above, a second model is needed for calculation of the airflow rate through the door opening with the use of this stop angle. Numerous empirical and semi-empirical models have been developed to investigate the impact of various factors on the airflow rate through a door or window opening. For instance, Yang et al. [12] used measured data from a small-scale wind tunnel test to develop an empirical equation for calculating the airflow rate through a door with different opening angles. Chu and Wang [13] developed an empirical correlation to assess the impact of door-to-wall area ratio on the airflow rate through a door opening. Chen et al. [14] considered the influence of the indoor-outdoor temperature differential in calculating the airflow rate through a door opening. Each of these models accounts for a single factor, e.g., the door opening angle, door-to-wall area ratio, or temperature differential, in addition to the pressure differential and door size. The present study developed a more generic, integrated model that accounts for all the factors mentioned above, including the indoor-outdoor pressure differential, door size, door opening angle, door-to-wall area ratio, and indoor-outdoor temperature differential.

The model is based on the orifice equation [15, 16]:

$$Q = C_d A \sqrt{\frac{2\Delta P}{\rho}} \tag{4}$$

where Q is the volumetric airflow rate (m^3/s), C_d is the discharge coefficient, A is the area of the door (m^2), ΔP is the indoor-outdoor pressure differential (Pa), and ρ is the air density (kg/m^3). The relationship between the discharge coefficient and the opening angle can be

described by the following empirical correlation [12]:

$$C_d = \begin{cases} 0.0256 \cdot \theta^{0.7432} & \theta < \theta^{\#} \\ C_d^{\#} & \theta \geq \theta^{\#} \end{cases} \tag{5}$$

where θ is the door opening angle (°), and $\theta^{\#}$ is the cutoff angle (°). When the door opening angle is larger than the cutoff angle, the discharge coefficient becomes a constant [12]. The cutoff angle can be determined by:

$$\theta^{\#} = \left(\frac{C_d^{\#}}{0.0256}\right)^{1.3455} \tag{6}$$

where $C_d^{\#}$ is the discharge coefficient when the door opening angle is sufficiently large. It was found that $C_d^{\#}$ is a function of the door-to-wall area ratio, which can be expressed by [13]:

$$C_d^{\#} = \begin{cases} \left(2.58\left(1-\exp\left(-60\frac{A}{A_{wall}}\right)\right)\right)^{-0.5} & \frac{A}{A_{wall}} < 10\% \\ 0.62 & \frac{A}{A_{wall}} \geq 10\% \end{cases} \tag{7}$$

where A_{wall} is the area of the wall where the door is installed (m^2). This correlation shows that when the door-to-wall area ratio (A/A_{wall}) is greater than 10%, the $C_d^{\#}$ is a constant. Numerous experimental measurements have confirmed that this constant is approximately 0.62 [12, 13, 17-19].

Note that Eqs. (4) through (7) apply only when there is no indoor-outdoor temperature differential. When a temperature differential exists, the buoyancy effect could cause two-way airflow through the door opening [14, 20, 21]. The airflow rate through a door opening driven by both a pressure differential and the buoyancy effect can be calculated by [14, 22]:

$$Q = \begin{cases} \frac{2}{3} W C_d \sqrt{\frac{2g\Delta\rho}{\rho}} \left(\frac{H}{2} + Y_n\right)^{\frac{3}{2}} - \frac{2}{3} W C_d \sqrt{\frac{2g\Delta\rho}{\rho}} \left(\frac{H}{2} - Y_n\right)^{\frac{3}{2}} & Y_n > \frac{H}{2} \\ \frac{2}{3} W C_d \sqrt{\frac{2g\Delta\rho}{\rho}} \left(\frac{H}{2} + Y_n\right)^{\frac{3}{2}} & Y_n \leq \frac{H}{2} \end{cases} \tag{8}$$

where W is the width of the door (m); H is the height of the door (m); g is the gravitational acceleration (m/s^2); $\Delta\rho$ is the indoor-outdoor air density differential (kg/m^3), which is a function of the indoor and outdoor temperatures; and Y_n is the distance between the neutral height and the height at H/2 (m), which can be calculated by [14]:

$$Y_n = \left| \frac{\Delta P}{g \Delta \rho} \right| \tag{9}$$

In this study, it was assumed that when the temperature differential is lower than 1 K, the impact of the buoyancy effect is negligible. Thus, Eq. (4) was used when ΔT was less than 1 K, and Eq. (8) when ΔT was greater than or equal to 1 K.

2.3 Energy cost calculation

During the design phase, most of the detailed information about the building is not available. Therefore, the method for assessing the energy cost saving from using an effective door closer should be simple. This study made the following assumptions for the sake of simplicity. First, the buildings use electrically driven chillers to provide cooling, and the air handling unit consists of a cooling coil and an electric resistance re-heater. Second, the buildings use natural gas boilers to provide heating, and only the sensible heat was considered for the heating process. Finally, the increase in fan energy consumption because of the airflow through the door opening was neglected.

The cooling air handling process is shown on the psychrometric chart in Figure 6(a). For the baseline case, in which the door closer is able to fully close the door, the return air at state 2c and the outdoor air at state 1 mix together to state 3c. The mixed air is then cooled and dehumidified to state 4c, and finally reheated to state 5c as the supply air. For the baseline case, the annual cooling energy cost can be calculated by:

$$Cost_{cool,baseline} = \sum_{i=1}^{8760} \frac{Prc_{elc}}{3600} \left[\frac{\rho(V_2 + V_1)(h_{3c,i} - h_{4c})}{COP} + \frac{\rho(V_2 + V_1)(h_{5c} - h_{4c})}{\eta_{reheat}} \right] \tag{10}$$

where Prc_{elc} is the price of electricity ($/kWh); ρ is the air density (kg/m^3); V_2 is the volume of return air (m^3); V_1 is the volume of outdoor air (m^3); h_{4c} and h_{5c} are the enthalpy of air leaving cooling coil and supplied to the room (kJ/kg), respectively; COP is the coefficient of performance of the chiller; and η_{reheat} is the efficiency of the electric resistance re-heater. The variable $h_{3c,i}$ is the enthalpy of mixed air in the ith hour of the year (kJ/kg) for the baseline case, which can be calculated by:

$$h_{3c,i} = \frac{V_2 h_{2c} + V_1 h_{1,i}}{V_2 + V_1} \tag{11}$$

where h_{2c} is the enthalpy of the return air (kJ/kg), and $h_{1,i}$ is the enthalpy of the outdoor air in the ith hour of the year (kJ/kg). For the actual case, in which the door closer may not be able to fully close the door, additional outdoor air is needed to make up for the air lost through the door opening. In this case, the return air at state 2c and more outdoor air at state 1 mix

together to state 3c'. The mixed air is then cooled and dehumidified to state 4c, and finally reheated to state 5c as the supply air. For the actual case, the annual cooling energy cost can be calculated by:

$$\mathrm{Cost}_{\mathrm{cool,actual}} = \sum_{i=1}^{8760} \frac{\mathrm{Prc}_{\mathrm{elc}}}{3600} \left[\frac{\rho(V_2 + V_1 + \Delta V_{1,i})(h_{3c',i} - h_{4c})}{\mathrm{COP}} + \frac{\rho(V_2 + V_1 + \Delta V_{1,i})(h_{5c} - h_{4c})}{\eta_{\mathrm{reheat}}} \right] \tag{12}$$

where $\Delta V_{1,i}$ is the volume of additional outdoor air that makes up for the air lost through the door opening in the i^{th} hour of the year (m^3), and $h_{3c',i}$ is the enthalpy of mixed air in the i^{th} hour of the year (kJ/kg) for the actual case, which can be calculated by:

$$h_{3c',i} = \frac{V_2 h_{2c} + (V_1 + \Delta V_{1,i}) h_{1,i}}{V_2 + V_1 + \Delta V_{1,i}} \tag{13}$$

The annual cooling energy cost saving from using an effective door closer can then be calculated by:

$$\mathrm{Cost}_{\mathrm{cool,saving}} = \mathrm{Cost}_{\mathrm{cool,actual}} - \mathrm{Cost}_{\mathrm{cool,baseline}} \tag{14}$$

Solving Eqs. (10) to (14) together, one finds that:

$$\mathrm{Cost}_{\mathrm{cool,saving}} = \sum_{i=1}^{8760} \frac{\mathrm{Prc}_{\mathrm{elc}}}{3600} \left[\frac{\rho \Delta V_{1,i}(h_{1,i} - h_{4c})}{\mathrm{COP}} + \frac{\rho \Delta V_{1,i}(h_{5c} - h_{4c})}{\eta_{\mathrm{reheat}}} \right] \tag{15}$$

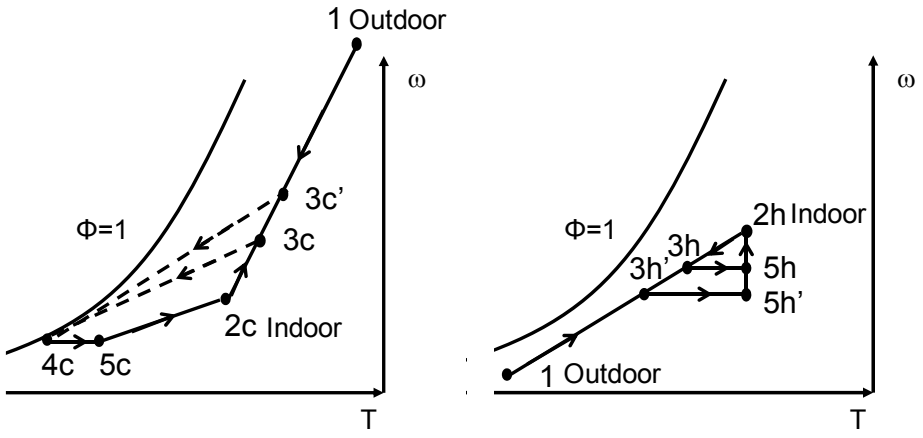

Figure 6. Psychrometric charts for the HVAC system considered in this study: (a) cooling and (b) heating.

The heating air handling process is shown on the psychrometric chart in Figure 6(b). Only the sensible heat was considered for the heating process, and the energy cost for operation of the humidifier was not considered. For the baseline case, in which the door closer is able to fully close the door, the return air at state 2h and the outdoor air at state 1 mix together to state 3h. The mixed air is then heated to state 5h as the supply air. For the baseline case, the annual heating energy cost can be calculated by:

$$\mathrm{Cost}_{\mathrm{heat,baseline}} = \sum_{i=1}^{8760} \frac{\mathrm{Prc}_{\mathrm{ng}}}{3600\mathrm{HV}_{\mathrm{ng}}} \frac{\rho c_p (V_2 + V_1)(T_{5h} - T_{3h,i})}{\eta} \tag{16}$$

where $\mathrm{Prc}_{\mathrm{ng}}$ is the price of natural gas ($/m^3), $\mathrm{HV}_{\mathrm{ng}}$ is the heating value of natural gas (kWh/m^3), c_p is the specific heat of air (kJ/kgK), T_{5h} is the supply air temperature during the heating season (K), and η is the efficiency of the natural gas boiler. The variable $T_{3h,i}$ is the temperature of mixed air in the ith hour of the year (K) for the baseline case, which can be calculated by:

$$T_{3h,i} = \frac{V_2 T_{2h} + V_1 T_{1,i}}{V_2 + V_1} \tag{17}$$

where T_{2h} is the temperature of the return air (K), and $T_{1,i}$ is the temperature of the outdoor air in the ith hour of the year (K). For the actual case, in which the door closer may not be able to fully close the door, the return air at state 2h and more outdoor air at state 1 mix together to state 3h'. The mixed air is then heated to state 5h as the supply air. For the actual case, the annual heating energy cost can be calculated by:

$$\mathrm{Cost}_{\mathrm{heat,actual}} = \sum_{i=1}^{8760} \frac{\mathrm{Prc}_{\mathrm{ng}}}{3600\mathrm{HV}_{\mathrm{ng}}} \frac{\rho c_p (V_2 + V_1 + \Delta V_{1,i})(T_{5h} - T_{3h',i})}{\eta} \tag{18}$$

where $T_{3h',i}$ is the temperature of the mixed air in the ith hour of the year (K) for the actual case, which can be calculated by:

$$T_{3h',i} = \frac{V_2 T_{2h} + (V_1 + \Delta V_{1,i}) T_{1,i}}{V_2 + V_1 + \Delta V_{1,i}} \tag{19}$$

The annual heating energy cost saving from using an effective door closer can then be calculated by:

$$\mathrm{Cost}_{\mathrm{heat,saving}} = \mathrm{Cost}_{\mathrm{heat,actual}} - \mathrm{Cost}_{\mathrm{heat,baseline}} \tag{20}$$

Solving Eqs. (16) to (20) together leads to the following expression:

$$\mathrm{Cost}_{\mathrm{heat,saving}} = \sum_{i=1}^{8760} \frac{\mathrm{Prc}_{\mathrm{ng}}}{3600\mathrm{HV}_{\mathrm{ng}}} \frac{\rho c_p \Delta V_{1,i}(T_{5h} - T_{1,i})}{\eta} \tag{21}$$

In Eqs. (15) and (21), the volume of additional outdoor air that makes up for the air lost through the door opening in the i^{th} hour of the year, $\Delta V_{1,i}$, needs to be determined. This study assumed that the door opening/closing cycles, when the door is being operated, are the same for the baseline and actual cases. Therefore, the difference in airflow volume through the door opening occurs when the door is not being used. The volume of additional outdoor air that makes up for the air lost through the door opening in the i^{th} hour of the year can then be calculated by:

$$\Delta V_{1,i} = (3600 - n_i t^*) Q_i \tag{22}$$

where 3600 represents the number of seconds in an hour, n_i is the number of times that the door is opened in the i^{th} hour of the year (#), t^* is the duration of a door opening/closing cycle when the door is being operated (s), and Q_i is the airflow rate through the door opening (m^3/s). The number of times that the door is opened in the i^{th} hour of the year, n_i, was based on the door opening schedule established by Cho et al. [6]. Table 7 of Cho et al. [6] provides the schedule for weekdays and weekends for a small office, medium office, warehouse, standalone retail store, strip mall, primary school, secondary school, quick-service restaurant, sit-down restaurant, outpatient health care facility, small hotel, and mid-rise apartment building. It was assumed that if the door cannot be fully closed, it remains at the stop angle only during the hours when the occupancy is not zero. To determine t^*, this study conducted field measurements for 481 door opening/closing cycles. Data acquisition systems were used to automatically record the door opening angle as a function of time for doors with effective closers. The measurement results showed that the average time for a cycle was 7 s. The variable Q_i is a function of stop angle, door size, indoor-outdoor pressure differential, door-to-wall area ratio, and indoor-outdoor temperature differential, which can be calculated using the airflow model described in Section 2.2 (Eqs. (4) through (9)). The stop angle, θ^*, can be determined by use of the stop angle model described in Section 2.1 (Eqs. (1) through (3)).

Finally, the total annual heating and cooling energy cost saving from using an effective door closer can be calculated by:

$$\mathrm{Cost}_{\mathrm{saving}} = \mathrm{Cost}_{\mathrm{cool,saving}} + \mathrm{Cost}_{\mathrm{heat,saving}} \tag{23}$$

Note that the energy cost calculation method proposed in this study is for use in the design phase when detailed information about the building is unavailable. The energy cost assessment will inform the designers about the reduction in heating and cooling energy costs

that can be achieved with the use of an effective door closer. In the design phase, such information can guide decisions about whether or not to use door closers in a building, and what kind of closer to use.

3. Model validation

3.1 Experimental setup

To validate the airflow model and stop angle model, this study conducted experimental measurements in a full-scale two-room test facility as shown in Figure 3. Again, Room 1 simulated the outdoor environment, while Room 2 simulated the indoor environment. A variable-speed fan system was used to exhaust air from Room 1, which created a pressure differential between the "indoor" and "outdoor" environments. The door-to-wall area ratio was 0.09. This study measured nine sets of airflow rates through the door opening under various pressure differentials and door opening angles, as listed in Table 1.

Table 1. Case setup and measured data for airflow measurements.

Case No.	Opening angle, θ (°)	Pressure differential, ΔP (Pa)	Measured airflow rate, Q (m^3/s)
1	0.75	7.7	0.16
2	1.25	6.9	0.18
3	2.5	1.3	0.13
4	2.5	3.3	0.22
5	2.5	4.4	0.26
6	3.75	1.1	0.17
7	3.75	1.8	0.23
8	5	1.2	0.22
9	7.5	0.7	0.22

Before each set of experiments, the rooms were ventilated using the fan system for two hours so that the temperatures in the two rooms were the same. This temperature equivalency allowed isolation of the impact of buoyancy on airflow through the door. Next, the door was opened at a given angle by the use of a doorstop. The pressure differential was controlled by adjusting the frequency of the fan. A manometer with an accuracy of 0.1 Pa was used to measure the pressure differential between the two rooms. The airflow rate was measured using the tracer gas decay method. Initially, a certain amount of the tracer gas sulfur hexafluoride (SF_6) was released into Room 2. Two mixing fans were used to ensure a uniform concentration of the tracer gas in the room air. A photo-acoustic multi-gas analyzer (INNOVA 1312) with a multipoint sampler (INNOVA 1309) was used to measure the SF_6 concentration every 30 s with an accuracy of 0.001 ppm. To convert the measured tracer-gas concentration decay data, least-squares regression analysis was employed. From the mass balance of SF_6 in the room, the SF_6 concentration as a function of time can be expressed by [23]:

$$C_{SF_6}(t) = C_{SF_6}(0)\exp(-\frac{Q}{V}\cdot t) \tag{24}$$

where $C_{SF6}(0)$ is the initial SF_6 concentration, and V is the volume of Room 2, which was

55.2 m^3. Figure 7 shows an example of the measured SF_6 tracer-gas concentration decay profile. By least-squares regression of the measured data the airflow rate through the door opening, Q, in Eq. (24) was obtained. The resulting airflow rates are listed in Table 1.

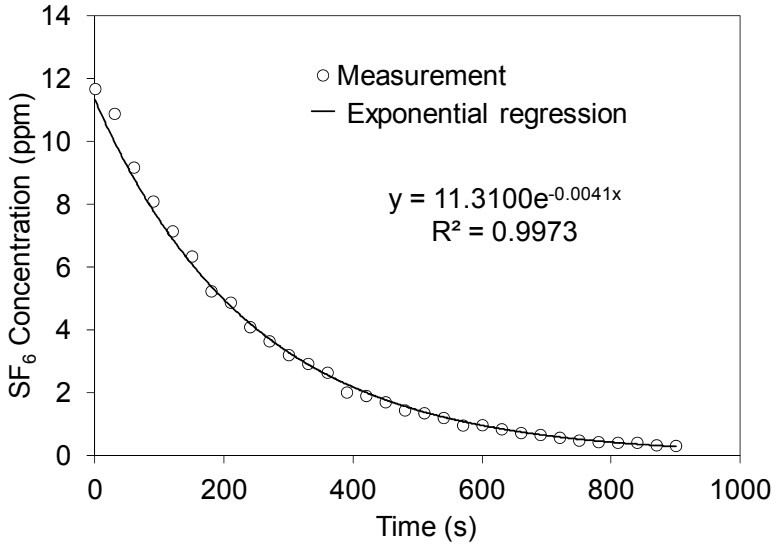

Figure 7. Example of the measured SF_6 tracer-gas concentration decay profile.

To validate the calculation method for pressure differential force, this study used a digital force gauge (Model Mark-10 Series EG) to measure the force on the door caused by the indoor-outdoor pressure differential. Under various pressure differentials and door opening angles, 10 sets of pressure differential forces on the door were measured. When the hinge was taken as the reference point, the corresponding pressure differential torque was obtained. Table 2 shows the case setup and measured data for the pressure differential torque. The measured data for both the airflow rate through the door opening and the torque on the door caused by the indoor-outdoor pressure differential were then used to validate the airflow model and stop angle model.

Table 2. Case setup and measured data for pressure differential torque measurements.

Case No.	Opening angle, θ (°)	Pressure differential when door fully closed, $\Delta P(0)$ (Pa)	Measured pressure differential torque, $\tau_{\Delta P}$ (N·m)
1	2.5	9.2	2.7
2	2.5	7.3	2.3
3	2.5	8.3	2.7
4	3.75	9.2	1.5
5	3.75	5.7	0.9
6	3.75	8.3	1.3
7	3.75	10.3	1.7

8	5	6.7	0.7
9	5.9	11.4	0.9
10	7.5	6.7	0.3

3.2 Validation of the models

This investigation used both the experimental data measured in this study and data from the literature to validate the airflow model (Eqs. (4) through (9)). Figure 8 compares the calculated airflow rate through the door opening with the measured data. There were a total of 227 sets of data, including the experimental data from this study and that from Yang et al. [12], Chu and Wang [13], Heiselberg et al. [19], and Chen et al. [14]. The data were obtained from both small-scale tests [12, 13] and full-scale experiments ([14], [19], and this study) with various pressure differentials, door sizes, door opening angles, door-to-wall area ratios, and temperature differentials. As shown in Figure 8, the calculated airflow rate through the door opening agreed well with the measured data. The average relative error of the calculated airflow rate for the 227 cases was 7.4%.

This study also used the measured data to validate the model for calculating pressure differential torque (Eqs. (1) and (2)). Figure 9 compares the calculated pressure differential torque on the door with the measured data from our laboratory measurements. It can be seen that most of the data points are within the 10% error lines. The average relative error of the calculated pressure differential torque for the 10 cases was 4.9%. Therefore, the models could be used in the subsequent assessment of heating and cooling energy cost saving from the use of an effective door closer in the design phase.

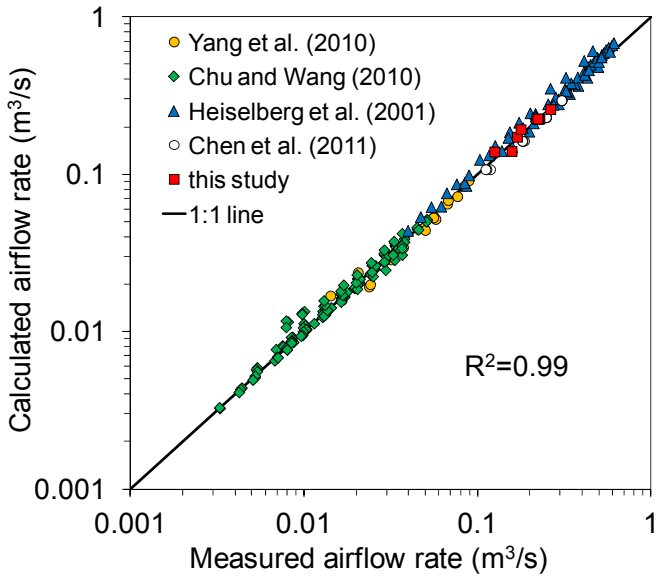

Figure 8. Comparison of calculated and measured airflow rates through door openings.

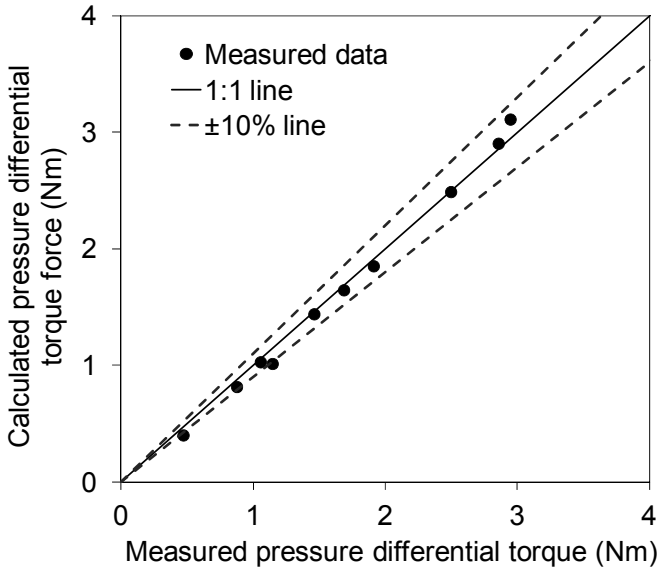

Figure 9. Comparison of calculated and measured pressure differential torque.

4. Case study

4.1 Case setup

This study applied the proposed method for assessing the heating and cooling energy cost saving from using an effective door closer to four cities in different climate zones: Minneapolis, Boston, San Francisco, and Phoenix. Minneapolis is in climate zone 6, which represents a very cold climate; Boston is in climate zone 5, which represents a cold climate; San Francisco is in climate zone 3, which represents a mild climate; and Phoenix is in climate zone 2, which represents a hot climate. The dimensions of the door were set at 2.2 m in height and 1.0 m in width, which were the average values from our field measurements of 15 doors. The ratio of door area to wall area was set at 0.12. The measurements showed that the indoor-outdoor pressure differential when the door was fully closed, $\Delta P(0)$, ranged from 3 to 26 Pa, with a median value of 12 Pa. Note that the measured indoor-outdoor pressure differentials have accounted for the impact of both the ventilation system and wind pressure. Four spring settings, closer size 0, closer size 1, closer size 2, and closer size 3 were tested. A medium-sized office was considered in this study as an example of a typical building. Details of the test cases are provided in Table 3.

Table 3. Details of the test cases.

Case No.	City	Door closer spring settings	Pressure differential when door fully closed, $\Delta P(0)$ (Pa)
1	Minneapolis	closer size 1	6
2	Minneapolis	closer size 1	8
3	Minneapolis	closer size 1	12
4	Minneapolis	closer size 1	18
5	Minneapolis	closer size 1	24
6	Minneapolis	closer size 0	12
7	Minneapolis	closer size 2	12

8	Minneapolis	closer size 3	12
9	Boston	closer size 1	6
10	Boston	closer size 1	8
11	Boston	closer size 1	12
12	Boston	closer size 1	18
13	Boston	closer size 1	24
14	Boston	closer size 0	12
15	Boston	closer size 2	12
16	Boston	closer size 3	12
17	San Francisco	closer size 1	6
18	San Francisco	closer size 1	8
19	San Francisco	closer size 1	12
20	San Francisco	closer size 1	18
21	San Francisco	closer size 1	24
22	San Francisco	closer size 0	12
23	San Francisco	closer size 2	12
24	San Francisco	closer size 3	12
25	Phoenix	closer size 1	6
26	Phoenix	closer size 1	8
27	Phoenix	closer size 1	12
28	Phoenix	closer size 1	18
29	Phoenix	closer size 1	24
30	Phoenix	closer size 0	12
31	Phoenix	closer size 2	12
32	Phoenix	closer size 3	12

The parameters for the energy calculation were set as follows. The COP was set at 3.0 for electrically driven chillers. The indoor temperature and relative humidity were set at 24 ^{o}C and 60%, respectively, in the cooling season. It was assumed that saturated air leaves the cooling coil at 12 ^{o}C. The cooled air is then reheated by an electric resistance heater with an efficiency of 100% and supplied to the room at 14 ^{o}C. Data for typical meteorological year 3 (TMY3) from the National Renewable Energy Laboratory [24] were used for the hourly outdoor temperature and relative humidity in a given city. The price of electricity was set at 0.109 $/kWh, which was the average price for commercial buildings across the U.S. in August of 2015 [25]. During the heating season, this study assumed that buildings are heated by natural gas boilers with an efficiency of 0.89. The indoor temperature was set at 21 ^{o}C and the supply air temperature at 26 ^{o}C. The price of natural gas was set at 0.39 $/m^3, which was the average value for commercial buildings across the U.S. in August of 2015 [26]. The heating value of natural gas is 10.35 kWh/m^3. The balance point temperature was used to determine the heating and cooling seasons. According to the U.S. National Oceanic and Atmospheric Administration, the calculation of heating degree days and cooling degree days typically uses a balance point temperature of 18.3 ^{o}C [27]. However, the balance point temperature may vary with the climate zone because of the building envelope insulation level. Note that calculation of this temperature requires information about building heating/cooling load, which may not be available during the design stage. Therefore, as a first approximation, the balance point temperatures were set at 19.8, 19.3, 18.8, 18.8, 14.4, 13.3, 11.1, and 11.1 ^{o}C,

respectively, for climate zones 1 through 8, on the basis of the different R-values recommended by ASHRAE [28] together with engineering judgment.

4.2 Results

Figure 10 shows the calculated annual energy cost saving from using an effective door closer under different pressure differentials in Minneapolis, Boston, San Francisco, and Phoenix when the door closer spring setting is closer size 1. Note that at the closer size 1 setting, it can normally be assumed that the force required to open the door to 70° is slightly less than 22 N. Therefore, it is worthwhile to explore the energy cost saving from using an effective closer at this spring setting. By use of the stop angle model, it was found that, at the spring setting of closer size 1, the door closer can fully close the door when ΔP(0) is less than or equal to 6 Pa. Therefore, for all four cities, when ΔP(0) is 6 Pa, there are no heating and cooling energy cost savings. Furthermore, under a greater indoor-outdoor pressure differential, using an effective door closer would save more energy cost. For example, when ΔP(0) increases to 24 Pa, using an effective closer could save $1695, $1478, $1140, and $879 in heating and cooling energy costs per door in Minneapolis, Boston, Phoenix, and San Francisco, respectively. This is because a greater indoor-outdoor pressure differential resulted in greater airflow through the door opening when using an ineffective door closer. In addition, the energy cost saving from using an effective door closer in San Francisco is lower than that in Minneapolis, Boston, and Phoenix. For instance, when ΔP(0) is 12 Pa, the energy cost saving in San Francisco is less than that in Minneapolis, Boston, and Phoenix by $556, $408, and $177, respectively. This difference can be attributed to the smaller indoor-outdoor temperature differential in mild-climate cities like San Francisco. With a smaller temperature differential, less energy is needed to condition the additional air flowing through the door opening.

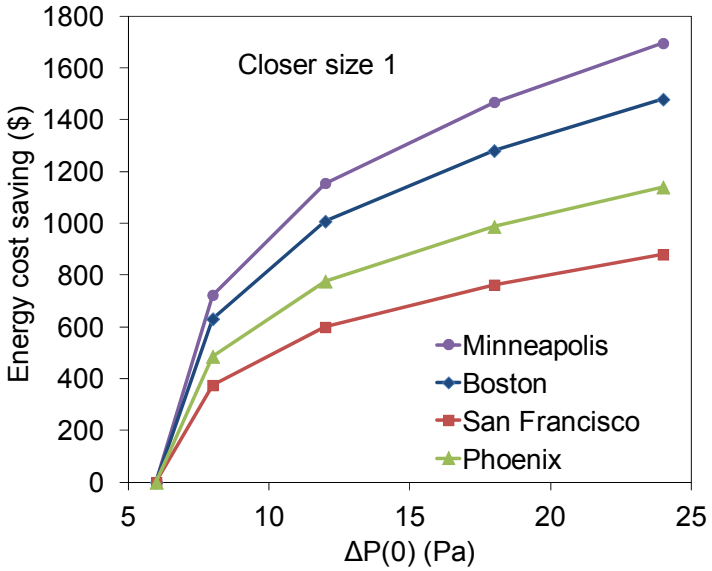

Figure 10. Calculated annual heating and cooling energy cost saving from using an effective door closer under different pressure differentials in Minneapolis, Boston, San Francisco, and Phoenix when the door closer spring setting is closer size 1.

Figure 11 shows the calculated annual energy cost saving from using an effective door closer under different door closer settings in Minneapolis, Boston, San Francisco, and Phoenix when ΔP(0) is 12 Pa. According to the stop angle model, when ΔP(0) is 12 Pa, the stop angles are 2.9°, 1.85°, and 0.95°, respectively, for the spring settings of closer size 0, closer size 1, and closer size 2. At the setting of closer size 3, the door closer can fully close the door under this pressure differential. Therefore, for all four cities, when the spring setting is closer size 3, there are no heating and cooling energy cost savings. Larger closer size corresponds to a greater amount of closing torque produced by the door closer, and therefore a smaller stop angle. Thus, when using a closer with a larger size, the energy cost lost would decrease because of the reduced airflow through the door opening. For example, in Phoenix, the spring setting of closer size 2 could save $199 more in heating and cooling energy costs than the closer size 1 setting. However, a larger closer size may increase the force required to open the door, reducing ease of use or in potential violation of the ADA standard [7]. Therefore, there is a tradeoff between energy cost saving and the accessiblity of the door.

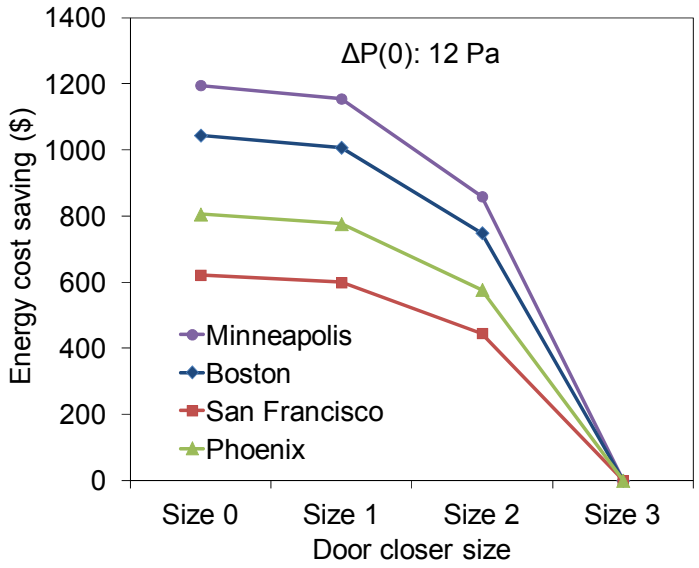

Figure 11. Calculated annual heating and cooling energy cost saving from using an effective door closer at different spring settings in Minneapolis, Boston, San Francisco, and Phoenix when ΔP(0) is 12 Pa.

5. Discussion

There are some limitations to the proposed method of assessing the heating and cooling energy cost saving from using an effective door closer. First, the method applies only to the design phase when detailed information about the building is unavailable. If designers would like to use this method at detailed later design stage, when the needed information is available, a comprehensive energy simulation should be performed using EnergyPlus or other software. Second, the indoor-outdoor pressure differential when the door is fully closed was set at the average value from the field measurements conducted in this study. The value may fluctuate throughout the year, but, since this method is for use in the design phase when detailed information about the building is unavailable, such an approximation should be acceptable.

Note that, when the indoor-outdoor pressure differential is negative, the door can always be fully closed. In this case, the energy cost lost associated with the door closer is no longer a problem. Finally, the proposed method provides only the calculated energy cost saving from using a door closer, which is just one part of the information needed by designers for selecting closers. Information about the security, accessibility, and cost of door closers is also required, but these factors were not included in this study.

The calculation of this study assumed that the door would be left open if the closer could not fully close the door. However, in real situation, some people may manually close the door, which would lower the actual energy lost because of using an ineffective door closer. It should be noticed that the purpose of using a door closer is to avoid the necessity of manually closing the door. Thus, it is not meaningful to include this factor into the calculation. Furthermore, this study mainly focused on casement doors because they are the most common type of doors used in daily life. In addition to casement doors, revolving, sliding, and other doors are also widely used in commercial buildings. For revolving or sliding doors, the energy cost lost associated with the door closers should not be a problem.

6. Conclusions

This study developed a method for assessing, in the design phase, the heating and cooling energy cost saving from using an effective door closer. The method consists of a stop angle model, an airflow model, and energy cost calculation. The stop angle is the angle at which the door remains open when the pressure differential force balances the closing force produced by a door closer. The airflow model can be used to calculate the airflow rate through a door opening, which accounts for various influencing factors. With the use of the calculated stop angles and airflow rates through the door opening as inputs, the energy cost calculation can provide information about the extent of energy cost saving from using an effective door closer. Within the scope of this study, the following conclusions can be made:

(1) The proposed airflow model and stop angle model predicted reasonably good results when compared with the experimental data.

(2) As the indoor-outdoor pressure differential increases from 6 to 24 Pa, the calcluated heating and cooling energy cost saving for office buildings in Minneapolis, Boston, Phoenix, and San Francisco would increase from $0 to $1695, $1478, $1140, and $879 per door, respectively.

(3) The cost saving from using an effective door closer in San Francisco (mild climate) would be lower than that in Minneapolis (very cold climate), Boston (cold climate), and Phoenix (hot climate). For instance, when $\Delta P(0)$ is 12 Pa, the energy cost saving for office buildings in San Francisco would be less than that in Minneapolis, Boston, and Phoenix by $556, $408, and $177, respectively.

(4) When using a closer with a larger size, the energy cost lost would decrease because of the reduced airflow through the door opening, but the large closing torques when the spring setting is more than closer size 1 may reduce ease of use and accessibility and violate the ADA standard.

Acknowledgements

The research presented in this paper was financially supported by Allegion plc.

References

[1] Energy Information Administration (EIA), Annual Energy Review, Washington, DC, 2011.
[2] S.J. Emmerich, A.K. Persily, Energy impacts of infiltration and ventilation in US office buildings using multi-zone airflow simulation, Proceedings of IAQ and Energy 98 (1998) 191-206.
[3] K. Gowri, D. Winiarski, and R. Jarnagin, Infiltration modeling guidelines for commercial building energy analysis, PNNL-18898, Pacific Northwest National Laboratory, Richland, WA. 2009.
[4] M. Shan, P. Wang, J. Li, G. Yue, X. Yang, Energy and environment in Chinese rural buildings: situations, challenges, and intervention strategies, Build. Environ. 91 (2015) 271-282.
[5] S.J. Emmerich, T. McDowell, W. Anis, Investigation of the impact of commercial building envelope airtightness on HVAC energy use. US Department of Commerce, Technology Administration, National Institute of Standards and Technology, (2005).
[6] H. Cho, K. Gowri, B. Liu, Energy saving impact of ASHRAE 90.1 vestibule requirements: Modeling of air infiltration through door openings, PNNL-20026, Pacific Northwest National Laboratory, Richland, WA. 2010.
[7] Americans with Disabilities Act (ADA), Standards for Accessible Design, 2010 Standards (2010).
[8] R.W. Dakhole, R.D. Askhedkar, S.K. Choudhary, Working of new design of door closer, Int. J. Mech. Eng. Rob. Res. 2 (2013) 400-406.
[9] F. Yildiz, Low-power energy harvesting from hydraulic door closer. J. Eng. Tech. 27 (2010) 18-25.
[10] J.-O. Lee, C.-S. Choi, Study on the assessment of the criteria on a door closer for the optimum design of the access door of a smoke control zone, J. Kor. Inst. Fire Sci. Eng. 27 (2013) 66-71.
[11] T.E. Waterman, Use of automatic door closers improves fire safety. J. Clin. Eng. 4 (1979) 260-264.
[12] C. Yang, H. Shi, X. Yang, B. Zhao, Research on flow resistance characteristics with different window/door opening angles, HVAC&R Res. 16 (2010) 813-824.
[13] C.-R. Chu, Y.-W. Wang, The loss factors of building openings for wind-driven ventilation, Build. Environ. 45 (2010) 2273-2279.
[14] C. Chen, B. Zhao, X. Yang, Impact of two-way air flow due to temperature difference on preventing the entry of outdoor particles using indoor positive pressure control method, J. Hazard. Mater. 186 (2011) 1290-1299.
[15] D. Etheridge, M. Sandberg, Building ventilation: Theory and measurement. John Wiley and Sons (1996).
[16] H.B. Awbi, Ventilation of buildings. 2nd ed. Taylor and Francis (2003).
[17] J.B. Dick, The fundamentals of natural ventilation of houses. J. Inst. Heat. Vent. Eng. 18 (1950) 123-134.

[18] E. Dascalaki, M. Santamouris, M. Bruant, C.A. Balaras, A. Bossaer, D. Ducarme, P. Woutersd, Modeling large openings with COMIS. Energy Build. 30 (1999) 105-115.
[19] P. Heiselberg, K. Svidt, P. Nielsen, Characteristics of airflow from open windows, Build. Environ. 36 (2001) 859-869.
[20] M. Caciolo, P. Stabat, D. Marchio, Full scale experimental study of single-sided ventilation: Analysis of stack and wind effects, Energy Build. 43 (2011) 1765-1773.
[21] J. von Grabe, Flow resistance for different types of windows in the case of buoyancy ventilation, Energy Build. 65 (2013) 516–522.
[22] CONTAMW, CONTAMW User's Manual, National Institute of Standards and Technology (NIST), Gaithersburg, MD, (2002).
[23] C. Chen, B. Zhao, W. Zhou, X. Jiang, Z. Tan, A methodology for predicting particle penetration factor through cracks of windows and doors for actual engineering application, Build. Environ. 47 (2012) 339-348.
[24] S. Wilcox, W. Marion, Users' manual for TMY3 data sets National Renewable Energy Laboratory (NREL). Vol. 43156. TP-581, (2008).
[25] Energy Information Administration (EIA), Electric Power Monthly. (2015). (http://www.eia.gov/electricity/monthly/epm_table_grapher.cfm?t=epmt_5_6_a)
[26] Energy Information Administration (EIA), Natural Gas Prices. (2015). (https://www.eia.gov/dnav/ng/ng_pri_sum_dcu_nus_m.htm)
[27] National Oceanic and Atmospheric Administration (NOAA), United States Climate Normals 1971–2000. Annual Degree Days to Selected Bases. Climatography of the United States No. 81. Supplement No. 2. Asheville, NC:NOAA. (2002).
[28] American Society of Heating, Refrigerating and Air-Conditioning Engineers (ASHRAE), ASHRAE Standards 90.1: Energy Standard for Buildings Except Low-Rise Residential Buildings, (2007).